International Journal of Civil Engineering (2019) 17:487–493
https://doi.org/10.1007/s40999-018-0310-3

RESEARCH PAPER

Nonlinear Seismic Response Analysis of High Arch Dams to Spatially-Varying Ground motions

Jin-Ting Wang[1] · Feng Jin[1] · Chu-Han Zhang[1]

Received: 14 November 2017 / Accepted: 30 April 2018 / Published online: 14 May 2018

Abstract
The failure of a large dam can be catastrophic to human life and property downstream. Therefore, the seismic safety is of particular concern for high dams in seismically active regions. This paper addresses the nonlinear seismic response analysis of high arch dams due to spatially-varying ground motions. Firstly, a comprehensive analysis model developed at Tsinghua University is presented, which takes into account radiation damping effect of semi-unbounded canyon, dynamic interaction of dam-water, opening of contraction joints, seismic damage cracking and strengthening of dam concrete, and nonlinearity of foundation rock. Subsequently, the seismic damage of Pacoima dam during the 1994 Northridge earthquake is qualitatively analyzed by the developed analysis model. The results agree with the actual damage observed after the earthquake. Most of the contraction joints opened and closed during the earthquake, and a larger residual opening occurred at the thrust block joint after the earthquake. The cracks continue from the bottom of the thrust block joint in three directions: diagonal, horizontal, and vertical. Finally, a large-scale numerical simulation of seismic ground motion from source rupture to dam canyon is introduced, which can simulate the characteristics of near-field ground motions at dam sites by considering the effect of source mechanism, propagation media, and local site.

Keywords Concrete dam · Seismic damage · Spatially-varying ground motion · Source to site

1 Introduction

Earthquakes can cause damage to dams, such as Xinfengjiang buttress dam (105 m high, 1962 Xinfengjiang earthquake), Koyna gravity dam (103 m high, 1967 Koyna earthquake), Pacoima arch dam (113 m high, 1971 San Fernando earthquake and 1994 Northridge earthquake), Rapel arch dam (112 m high, 1985 Rapel Lake earthquake), Sefid Rud buttress dam (106 m high, 1990 Manjil-Rudbar earthquake), Shihgang dam (25 m high, 1999 Chi–Chi earthquake), and Zhipingpu concrete-faced rockfill dam (156 m high, 2008 Wenchuan earthquake). Therefore, the seismic safety of dams is a widely-concerned topic. During last several decades, considerable research efforts have been devoted to seismic safety study of dams, and many numerical models have been developed to analyze seismic response of arch dams, such as [1–8]. However, due to the complexity of arch dam-reservoir-foundation rock systems, the numerical models are inevitably filled with assumptions. Determining the extent to which the developed numerical models may be truly representative of the actual systems is still a challenging problem.

A major difficulty lies in rationally defining the variations in ground motions along dam-foundation interfaces. The ground motions recorded at several arch dams, such as Pacoima dam [9], Mauvoisin dam [9] and Ertan dam [10], provide an opportunity to verify the effectiveness of numerical models. Chopra and Wang [9] investigated the linear response of Pacoima dam to the spatially-varying ground motions recorded during earthquakes. Wang et al. [5] investigated the earthquake damage of Pacoima dam in the 1994 Northridge earthquake of magnitude 6.7 using a comprehensive analysis model, which the semi-unbounded size of foundation rock and compressible water, the opening of contraction joints, the cracking of dam body, and the spatial variation of ground motions. The joint opening and the concrete cracking may be roughly reproduced when the ground motion excitation is spatially defined based on the acceleration records at the dam-rock interface.

✉ Jin-Ting Wang
wangjt@tsinghua.edu.cn

[1] Department of Hydraulic Engineering, Tsinghua University, Beijing 100084, China

However, most high dams, particularly new dams, lack appropriate strong motion records at dam-canyons for seismic safety evaluation. Recently, He et al. [11] and Wang et al. [12] investigated the ground motions at dam sites by numerically simulating the complete propagation process of seismic waves from fault rupture to dam site. The physics-based numerical simulation may take into account the effects of source, propagation path and local site, and thus offer a potential way for predicting ground motions at dam sites.

This paper summarizes some of the above-mentioned work. Firstly, a comprehensive analysis model developed at Tsinghua University is presented. Subsequently, the damage of Pacoima dam during the 1994 Northridge earthquake is qualitatively analyzed by the developed analysis model. Thirdly, a large-scale numerical simulation of seismic ground motion from source rupture to dam canyon is introduced.

2 Earthquake Damage Analysis model of Dam-Water-Foundation Systems

The arch dam-water-foundation rock system considered is composed of a concrete dam with contraction joints, semi-unbounded foundation rock, and semi-unbounded reservoir, as shown in Fig. 1. A comprehensive analysis model [5, 13–18] has been developed by the research group on earthquake resistance of high dams at Tsinghua University, which takes into account radiation damping effect of semi-unbounded canyon, dynamic interaction of dam-water, opening of contraction joints, seismic damage cracking and strengthening of dam concrete, and nonlinearity of foundation rock.

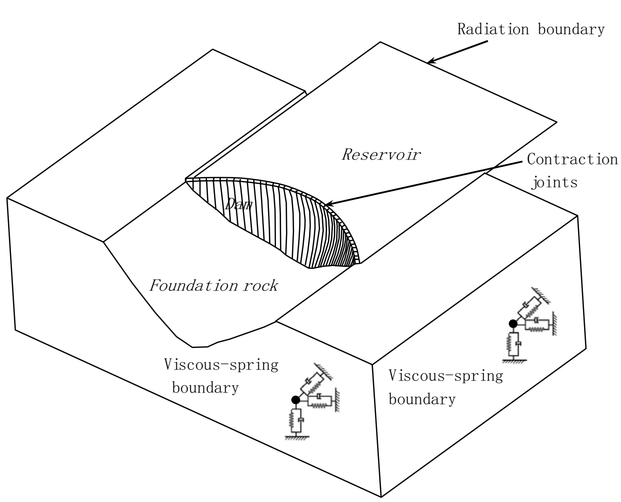

Fig. 1 Sketch of the arch dam-water-foundation rock system

1. Radiation damping model of semi-unbounded foundation rock

The semi-unbounded foundation rock is truncated in a certain region. Zhang et al. [13] applied the viscous-spring boundary condition [19] to the truncated foundation boundary to simulate the radiation damping of the semi-unbounded foundation rock. In the viscous-spring boundary input model, pairs of dashpots and springs are installed in all nodes of artificial boundaries as shown in Fig. 1. Each node on the artificial boundary contains three pairs of dashpots and springs, i.e. one in the normal direction of the boundary plane and the other two in the tangential directions. The parameters of springs and dashpots on the artificial boundary are given as the following:

$$K_{\mathrm{n}} = a \cdot \frac{\lambda + 2G}{r} \quad C_{\mathrm{n}} = b\rho V_{\mathrm{P}} \tag{1}$$

$$K_{\mathrm{s}} = a \cdot \frac{G}{r} \quad C_{\mathrm{s}} = b\rho V_{\mathrm{S}} \tag{2}$$

where the subscripts n and s refer to the normal and tangential directions of the artificial boundary surfaces; K is the elastic stiffness of the spring, C is the viscous damping, λ and G are the Lame's constants; V_{P} and V_{S} denote the propagation velocity of P- and S-waves, respectively; ρ is the mass density; r is the distance from the wave source, which takes the approximate value of the perpendicular distance from the center of the structure to the nodes of artificial boundary; and a and b are modification coefficients, which may be determined from parameter analysis.

2. Modeling of semi-unbounded reservoir

The impounded water is assumed to be inviscid, irrotational, and compressible. Similar to the semi-unbounded foundation rock, the semi-unbounded reservoir is truncated at a certain distance in the upstream direction. Wang et al. [15] used the plane-wave radiation condition at the truncated water boundary to simulate the fluid wave that propagates along the upstream direction. The plane-wave radiation equation [20] is expressed as

$$\frac{\partial p}{\partial n} = \frac{\cos\theta}{V_{\mathrm{w}}}\dot{p} \tag{3}$$

where p is the hydrodynamic pressure of the impounded water, and the superposed dot indicates the partial differentiation with respect to time; n is the inward normal direction of the truncated reservoir boundary; θ is the incident angle from the inward normal; and V_{w} is the velocity of pressure waves in the water.

3. Modeling of contraction joints

The nonlinear response of high-arch dams due to contraction joint opening during earthquakes is significant. It is of importance to appropriately model the behavior of interaction between monoliths. Zhang et al. [13] improved a contact boundary [21] provided in ABAQUS to simulate the opening-closing behavior of contraction joints.

4. Damage model of concrete

Dam concrete may crack during a strong earthquake because of excessive stress. For example, Pacoima dam suffered severe damage during the 1994 Northridge earthquake. Pan et al. [14] adopted the elastic–plastic damage model [22] to simulate the nonlinearity of concrete material during strong earthquakes. Considering that dam safety is usually controlled by tensile stresses during earthquakes, only the tensile damage of concrete is considered. Moreover, the compressive stiffness is assumed to fully recover upon the closure of cracks when load changes from tension to compression. Based on these assumptions, the uniaxial stress–strain relationship of concrete is shown in Fig. 2, where σ and ε are concrete stress and strain, respectively; E_0 is the initial (undamaged) elastic modulus; d_t is the tensile damage factor that varies from 0 (undamaged material with elastic behavior) to 1 (fully damaged material); G_f is the fracture energy; f_t is the tensile strength; ε_t and ε_f are the maximum elastic and limiting tensile strains, respectively; ε_p is the equivalent plastic strain; and l_c is the characteristic length of concrete (commonly defined as three times the maximum aggregate size).

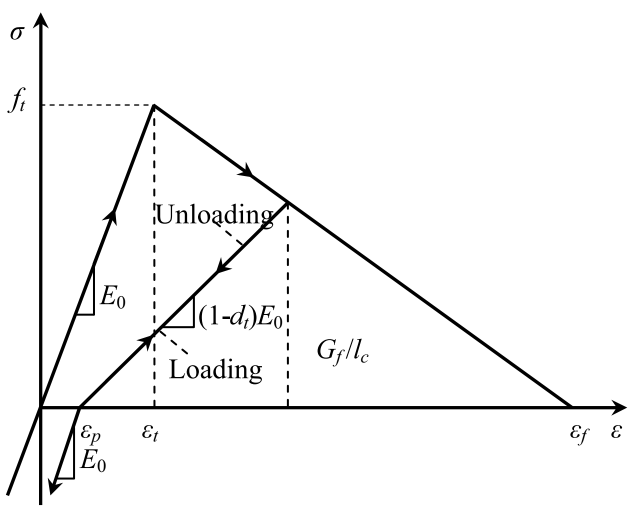

Fig. 2 Softening curve of concrete under uniaxial cyclic loading

5. Earthquake input model

Two earthquake input methods may be used in the dynamic analysis of arch dams to consider the radiation damping of semi-unbounded foundation rock [15]. As schematically shown in Fig. 3, one is the incident wave model, and the other is the free-field model. The incident wave model defines the seismic input at the foundation base boundary. To maintain the consistency of the motions at the base boundary with the specified free-field surface motions, the input excitation at the foundation base is usually determined by a deconvolution analysis. The incident wave is a uniform input at the base, but spatially varying ground motions are generated at the dam-foundation rock interface due to the scattering effect of canyon topography on the earthquake waves. In the free-field model, the specified free-field motions are imposed as direct input to the dam-foundation interface. Therefore, spatially varying free-field input could be considered if it is available. Wang et al. [5, 15] developed an equivalent force scheme to achieve the free-field input in the direct finite element analysis when the radiation damping of semi-unbounded foundation rock is taken into account. It is worth noting that the artificial boundary condition at the foundation base is essential in simulating the semi-unbounded of the foundation rock for these two input models in the finite element analysis.

Fig. 3 Earthquake input mechanism

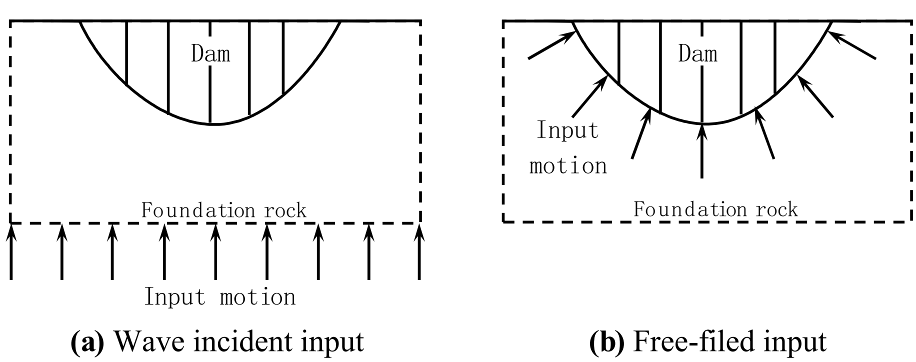

3 Earthquake Damage Analysis of Pacoima Dam

Located in the San Gabriel Mountains near Los Angeles, Pacoima dam is 113 m high and 180 m long at the crest. The thickness at the crown section varies from 3 m at the crest to 30 m at the base. A thrust block supports the dam at the left abutment. Pacoima dam was shaken by the 1971 San Fernando earthquake of magnitude 6.6 and the 1994 Northridge earthquake of magnitude 6.7. Figure 4 shows the observed damage of Pacoima dam in the Northridge earthquake [23]. The thrust block joint opened and remained open after the earthquake by about 50 mm at the crest level. This opening continued downward and decreased to 5 mm at the bottom of the joint. The rest of the contraction joints were closed after the earthquake. However, there were indications that some of joints opened and closed during the earthquake. A crack diagonally extended from the open joint through the thrust block into the abutment. Several fine cracks were also observed in the dam body adjacent to the thrust block. A permanent horizontal offset 10–15 mm occurred along the horizontal joint about 15 m below the crest. The top block moved downstream relative to the bottom block.

The seismic response of Pacoima dam to the 1994 Northridge earthquake is analyzed using the procedure presented in Sect. 2 [5]. The applied static loads include the deadweight of the dam, and the hydrostatic pressure of the reservoir. The ground motions that are spatially varied along the dam-foundation rock interface are defined based on the earthquake records [9]. Figure 5 presents the joint opening envelope, the residual joint opening, and the damage distribution on the downstream face during the earthquake excitation.

From Fig. 5, it is clearly observed that most of the joints are open during the earthquake. Some of the joints open downward about half the height of the dam. On the downstream face, the maximum opening 36.0 mm occurs at the crest level of the thrust block joint. The thrust block joint remains open about 15 mm at the crest level. This opening continues downward and decreases to 5 mm at the bottom. These scenarios are qualitatively similar to the actual observation after the 1994 Northridge earthquake, wherein some of the joints opened during the earthquake and the thrust block joint remained open after earthquake.

The calculated damage distribution (Fig. 5c) indicates that the severe damage occurs under the earthquake excitation. The damage appears in the dam body adjacent to the thrust block and to the foundation rock. The damage extends from the bottom of the thrust block joint in three directions. A crack diagonally extends from the bottom of the open joint into the left abutment. A crack horizontally stretches out from the open joint into the dam body. In addition, damage extends downwards along the vertical contraction joint. These damage modes agree with the actual cracks observed after the 1994 Northridge earthquake.

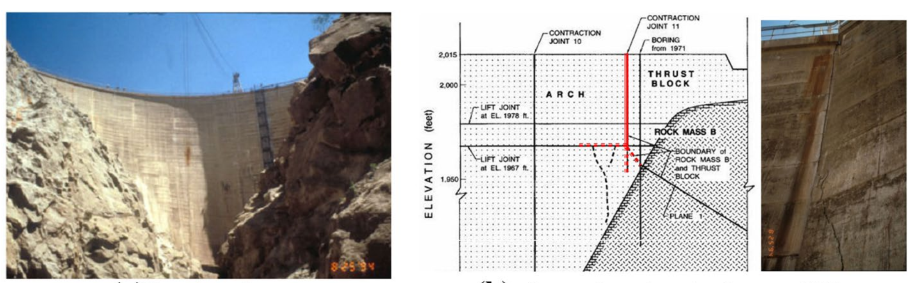

(a) Pacoima dam (b) observed earthquake damage [23]

Fig. 4 Observed damage of Pacoima dam in the Northridge earthquake

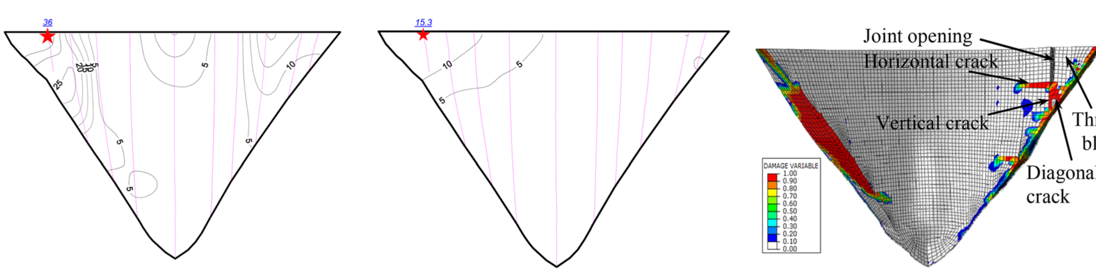

(a) Joint opening envelope (mm) (b) Residual joint opening (mm) (c) Damage distribution

Fig. 5 Computed response of Pacoima dam due to Northridge earthquake

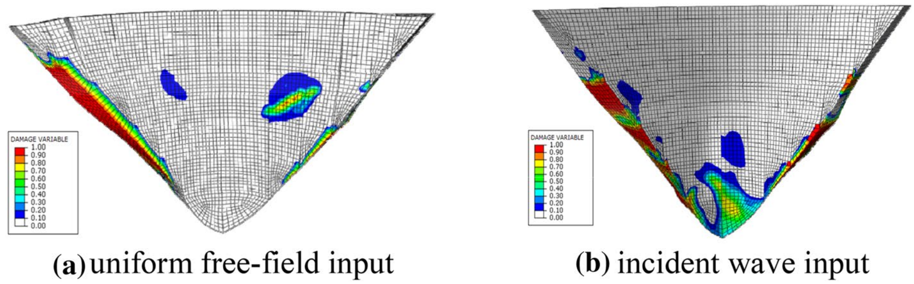

Fig. 6 Dam damage with different earthquake input mechanisms

Figure 6 shows the seismic damage on the downstream face of Pacoima dam when the input ground motion is defined by the two methods commonly-used in the current engineering practice, respectively. The first one is the free-field input, in which uniform ground motion is input at the dam-foundation interface. The second one is the incident wave input, in which the ground motion with the amplitude halved is vertically incident from the bottom of the foundation rock. It is obvious that the earthquake input mechanism has a significant influence on the damage distribution of Pacoima dam. The uniform free-field input and the incident wave input cannot achieve the damage mode that occurred during the 1994 Northridge earthquake.

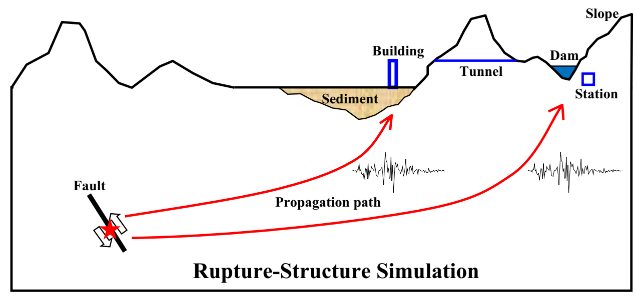

Fig. 7 Schematic of numerical simulation of seismic waves from source

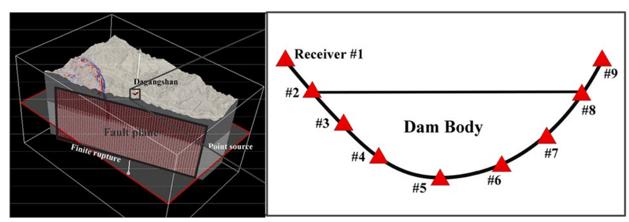

Fig. 8 Three dimensional numerical model of Dagangshan dam site

4 Large-Scale Numerical Simulation of Ground Motions at Dam Canyons

Ground motions recorded exhibit spatial variation along the dam-foundation interface, which may have a significant influence on the seismic response of high arch dams. From the seismic response analysis of Pacoima dam [5], it is clearly shown that the seismic responses resulting from the recorded ground motions are quite different compared with conventional assumptions. However, it is difficult to rationally define such variation in practice engineering because the available ground motions at the dam-foundation interface are limited.

With the significant improvements in the seismological methods, numerical simulation techniques and large-scale computing, it is promising to simulate the complete process of seismic waves from fault rupture to sites. Therefore, we proposed a "rupture-site" approach to generate spatially–varying ground motions along dam canyons [11, 12]. As schematically shown in Fig. 7, the fundamental idea is to build a realistic fine model integrated of seismic source, propagation path and local site to simulate the complete propagation process of the seismic wave from the fault rupture to the dam site based on large scale high-performance computing. This physics-based approach may take into account the effects of source mechanism, propagation path, and local site on the seismic response of dams, and thus predict ground motion for a specific dam.

Next, the ground motions at the Dagangshan dam site in Southwest China is simulated as an example [12]. The closest active fault is only 4.5 km away from the dam site, and it has an upper bound magnitude of M_W 7.4. Figure 8 shows the numerical model and 9 receivers deployed along the dam base. The rupture area is assumed to be 60 km in length and 28 km in width. From the profile of the fault, it can be seen that the whole rupture is discretized into an array of point sources and each point source represents a subfault. Both the velocity structure and surface topography are included in the simulation. Summaries of the global model information are as follows: $288 \times 240 \times 40$ spectral elements are distributed on 120 processors; the total DOFs add up to 0.54 billion; and the whole computation takes 2.7 h to finish 20,000 time steps.

Upon the numerical simulation, the acceleration time histories at all the nodes in the SEM model are computed in three components. The north components of the nine receivers deployed along the canyon are plotted in Fig. 9. It is apparent that the ground motions are different at the

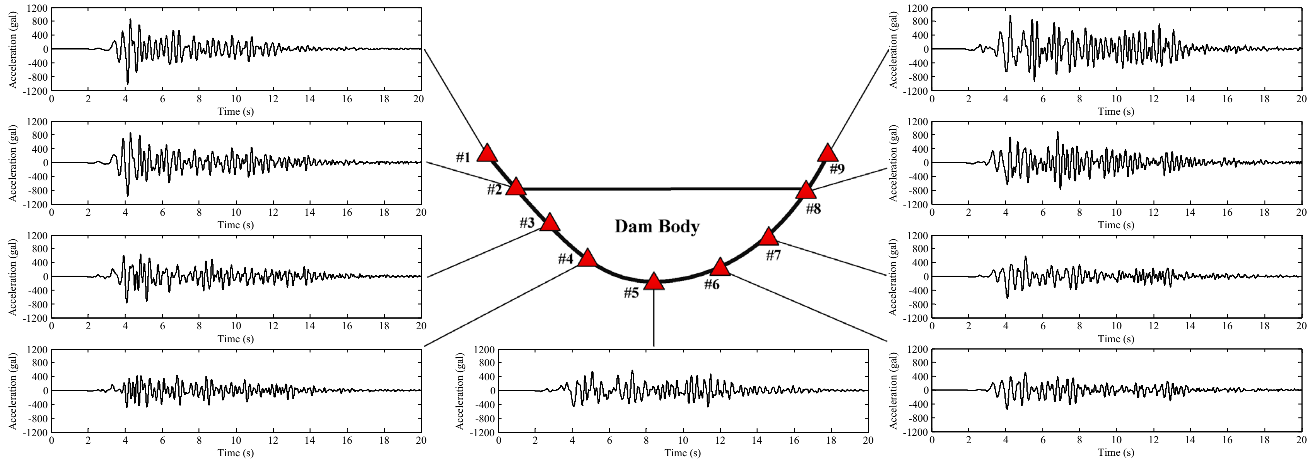

Fig. 9 North components of the nine receivers at dam canyon

9 receivers. The peak value of the north acceleration component at the bottom of the dam canyon (Receiver #5) is 593 cm/s^2. However, the east acceleration component has a peak value of 390 cm/s^2 at the same point. This indicates that ground motions vary along different directions. This phenomenon is conventionally not taken into consideration in earthquake-resistant design, which may have a significant effect on the seismic response of high dams.

5 Conclusions

The damage of Pacoima dam occurred in the 1994 Northridge earthquake is qualitatively reproduced by the comprehensive analysis model developed at Tsinghua University. This verifies the effectiveness of the analysis model. Therefore, we may conclude that the comprehensive analysis procedure can represent the real behavior of arch dams to a certain extent. One key issue is the spatially-varying ground motions along the dam-foundation interface, which has a significant influence on the seismic damage mode. However, the variation of ground motions along the dam-foundation is usually unavailable for most dams, particularly new dams under construction or planned.

The physics-based "rupture-site" approach can simulate the rupture process of the causative fault and take into account the velocity structure of propagation path and realistic topography, and thus predict site-specific ground motions for high dams. Therefore, it is a promising method for predicting the ground motions at dam sites due to maximum credible earthquake. However, the accuracy of the numerical simulation of seismic waves heavily relies on the models describing the source and propagation path. Therefore, more efforts are needed from researches in both seismological and engineering fields.

Acknowledgements The authors gratefully acknowledge the financial supports provided by the National Natural Science Foundation of China, under Granted nos. 51639006 and 51725901. Appreciation is expressed to Prof. Yan-Jie Xu and Dr. Jian-Wen Pan for their valuable discussion and suggestions. The authors are also grateful to Professor Anil K. Chopra, University of California at Berkeley, for helpful advice and comments on the earthquake input models.

References

1. Zhang C, Jin F, Pekau OA (1995) Time Domain procedure of FE-BE-IBE coupling for seismic interaction of arch dams and canyon. Earthq Eng Struct Dyn 24:1651–1666
2. Maeso O, Aznarez JJ, Dominguez J (2004) Three-dimensional models of reservoir sediment and effects on the seismic response of arch dams. Earthq Eng Struct Dyn 33(10):1103–1123
3. Du X, Tu J (2007) Nonlinear seismic response analysis of arch dam-foundation systems-part II opening and closing contact joints. Bull Earthq Eng 5:121–133
4. Wang J, Chopra AK (2010) Linear analysis of concrete arch dams including dam-water-foundation rock interaction considering spatially varying ground motions. Earthq Eng Struct Dyn 39(7):731–750
5. Wang J, Lv D, Jin F, Zhang C (2013) Earthquake damage analysis of arch dams considering dam-water-foundation interaction. Soil Dyn Earthq Eng 49:64–74
6. Alembagheri M, Ghaemian M (2013) Damage assessment of a concrete arch dam through nonlinear incremental dynamic analysis. Soil Dyn Earthq Eng 44:127–137
7. Mircevska V, Nastev M, Hristovski V, Bulajic I (2014) Arch dam-fluid interaction considering reservoir topology. J Earthq Eng 18(7):1083–1101
8. Omidi O, Lotfi V (2017) Seismic plastic–damage analysis of mass concrete blocks in arch dams including contraction and peripheral joints. Soil Dyn Earthq Eng 95:118–137
9. Chopra AK, Wang J (2010) Earthquake response of arch dams to spatially-varying ground motion. Earthq Eng Struct Dyn 39(8):887–906
10. Yang J, Jin F, Wang J, Kou L (2017) System identification and modal analysis of an arch dam based on earthquake response records. Soil Dyn Earthq Eng 92:109–121

11. He C, Wang J, Zhang C, Jin F (2015) Simulation of broadband seismic ground motions at dam canyons by using a deterministic numerical approach. Soil Dyn Earthq Eng 76:136–144
12. Wang J, He C, zhang C (2017) Large-scale wave propagation simulation from fault rupture to dam structures. In: Proceedings of 16th World Conference on Earthquake Engineering, Paper No. 3311, Santiago Chile
13. Zhang C, Pan J, Wang J (2009) Influence of seismic input mechanisms and radiation on arch dam response. Soil Dyn Earthq Eng 29(9):1282–1293
14. Pan J, Zhang C, Wang J, Xu Y (2009) Seismic damage-cracking analysis of arch dams using different earthquake input mechanisms. Sci China Ser E Technol Sci 52:518–529
15. Wang J, Zhang C, Jin F (2012) Nonlinear earthquake analysis of high arch dam-water-foundation rock systems. Earthq Eng Struct Dyn 41(7):1157–1176
16. Long Y, Zhang C, Jin F (2008) Numerical simulation of reinforcement strengthening for high-arch dams to resist strong earthquakes. Earthq Eng Struct Dyn 37:1739–1761
17. Pan J, Xu Y, Jin F, Wang J (2015) Seismic stability assessment of an arch dam-foundation system. Earthq Eng Eng Vib 14(3):517–526
18. Song L, Wu M, Wang J, Xu Y (2016) Seismic damage analysis of the outlet piers of arch dams using the finite element sub-model method. Earthq Eng Eng Vib 15(3):617–626
19. Liu J, Li B (2005) A unified viscous-spring artificial boundary for 3-D static and dynamic applications. Sci China Ser E Eng Mater Sci 48(5):570–584
20. ABAQUS Inc (2007) Abaqus theory manual. Version 6.7. ABAQUS, Inc., Providence
21. Bathe KJ, Chaudhary A (1985) A solution method for planar and axisymmetric contact problems. Int J Numer Methods Eng 21(1):65–88
22. Lee JL, Fenves GL (1998) Plastic-damage model for cyclic loading of concrete structures. J Eng Mech ASCE 124(3):892–900
23. Ghanaat Y (2004) Failure modes approach to safety evaluation of dams. In: Proceedings of 13th World Conference on Earthquake Engineering, Paper No. 1115, Vancouver, Canada